

Supplementary Information for: Combining fine-scale social contact data with epidemic modelling reveals interactions between contact tracing, quarantine, testing and physical distancing for controlling COVID-19

Josh A. Firth^{1,2}, Joel Hellewell³, Petra Klepac^{3,4}, Stephen Kissler⁵, CMMID COVID-19 working group, Adam Kucharski³, Lewis G. Spurgin^{6*}

1. Department of Zoology, University of Oxford, Oxford, UK
2. Merton College, University of Oxford, Oxford, UK
3. Centre for the Mathematical Modelling of Infectious Diseases, Department of Infectious Disease Epidemiology, London School of Hygiene & Tropical Medicine, London, UK
4. Department for Applied Mathematics and Theoretical Physics, University of Cambridge
5. Department of Immunology and Infectious Diseases, Harvard T.H. Chan School of Public Health, Boston MA
6. School of Biological Sciences, University of East Anglia, Norwich, UK

*Correspondence: l.spurgin@uea.ac.uk

CMMID COVID-19 working group members (order selected at random): Mark Jit, Katherine E. Atkins, Samuel Clifford, C Julian Villabona-Arenas, Sophie R Meakin, Charlie Diamond, Nikos I Bosse, James D Munday, Kiesha Prem, Anna M Foss, Emily S Nightingale, Kevin van Zandvoort, Nicholas G. Davies, Hamish P Gibbs, Graham Medley, Amy Gimma, Stefan Flasche, David Simons, Megan Auzenbergs, Timothy W Russell, Billy J Quilty, Eleanor M Rees, Quentin J Leclerc, W John Edmunds, Sebastian Funk, Rein M G J Houben, Gwenan M Knight, Sam Abbott, Fiona Yueqian Sun, Rachel Lowe, Damien C Tully, Simon R Procter, Christopher I Jarvis, Akira Endo,

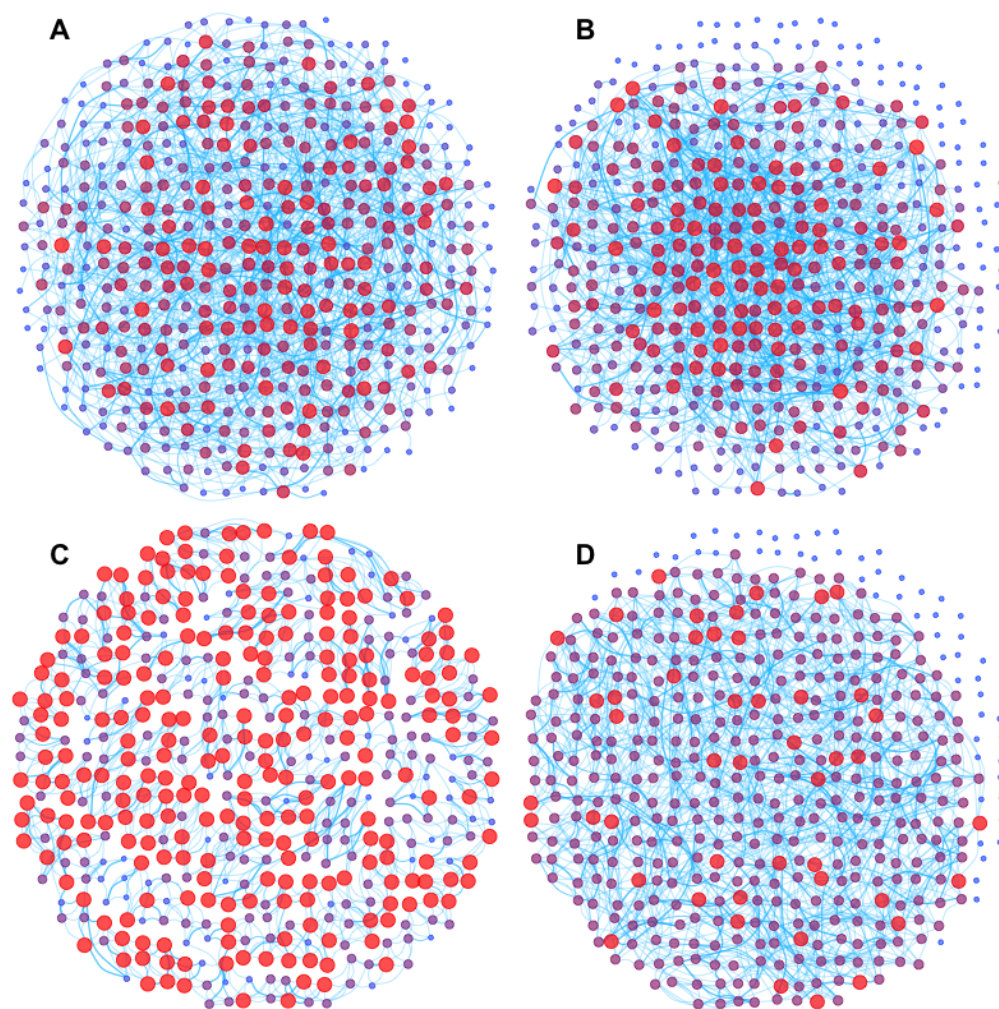
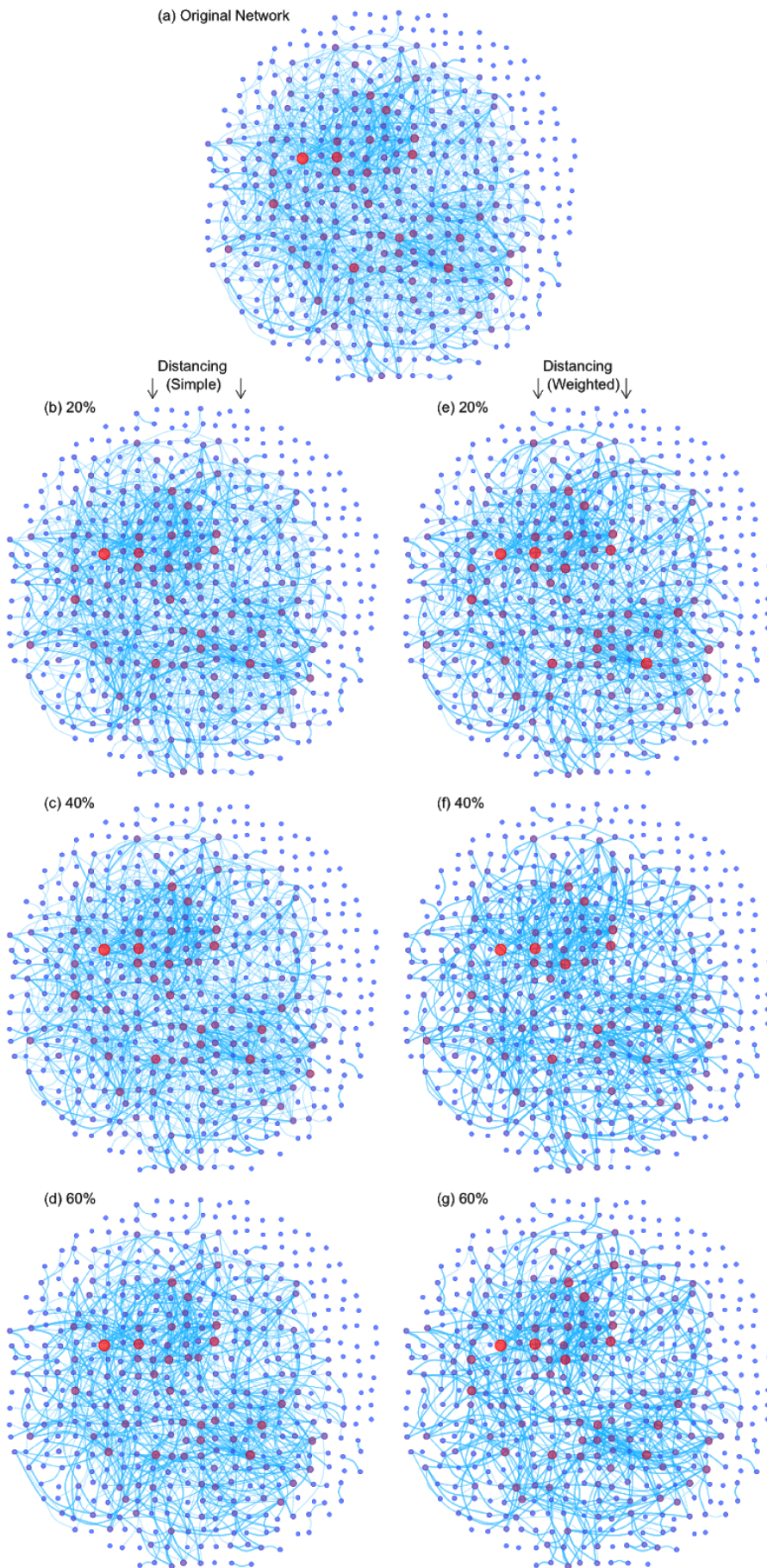


Figure S1 Graphical depiction of examples of the networks of social contact generated under the four different empirically parameterised null models. Number of unique contact partners is denoted by size and colour of nodes (large & red = central) with this standardised within each panel (max node size = 3x min node size). Each panel contains the same number of unique edges in total, and the strength of the edges (denoted by thickness) is also maintained. The panel order follows that of main text Figure 3, with **A** edge null, **B** degree null, **C** lattice null and **D** cluster null (see methods for details). Each network is organised in a fitted spring layout which is then rescaled into an equally-spaced filled circular format.

Figure S2 Graphical depiction of examples of social networks under the two different physical distancing criteria.

Number of unique contact partners is denoted by size and colour of nodes (large & red = central) with this standardised within each panel (max node size = 3x min node size). Each panel contains the same sum of weighted edges in total, but the number of unique edges (occurring on just one day) is reduced as these are reassigned to other existing edges. The panels show (A) the observed social network, (B, C and D) physical distancing scenario 1 at 20%, 40% and 60%, where edges that occurred on just one day



are simply reassigned to other edges, and (E, F, G) physical distancing scenario 2 at 20%, 40% and 60% where reassignment is based on the total amount of time (5min intervals) that each dyad was in contact (see methods for details). Each network is in the same format across panels, which is a spring layout of the observed network then rescaled into an equally spaced filled circular format.

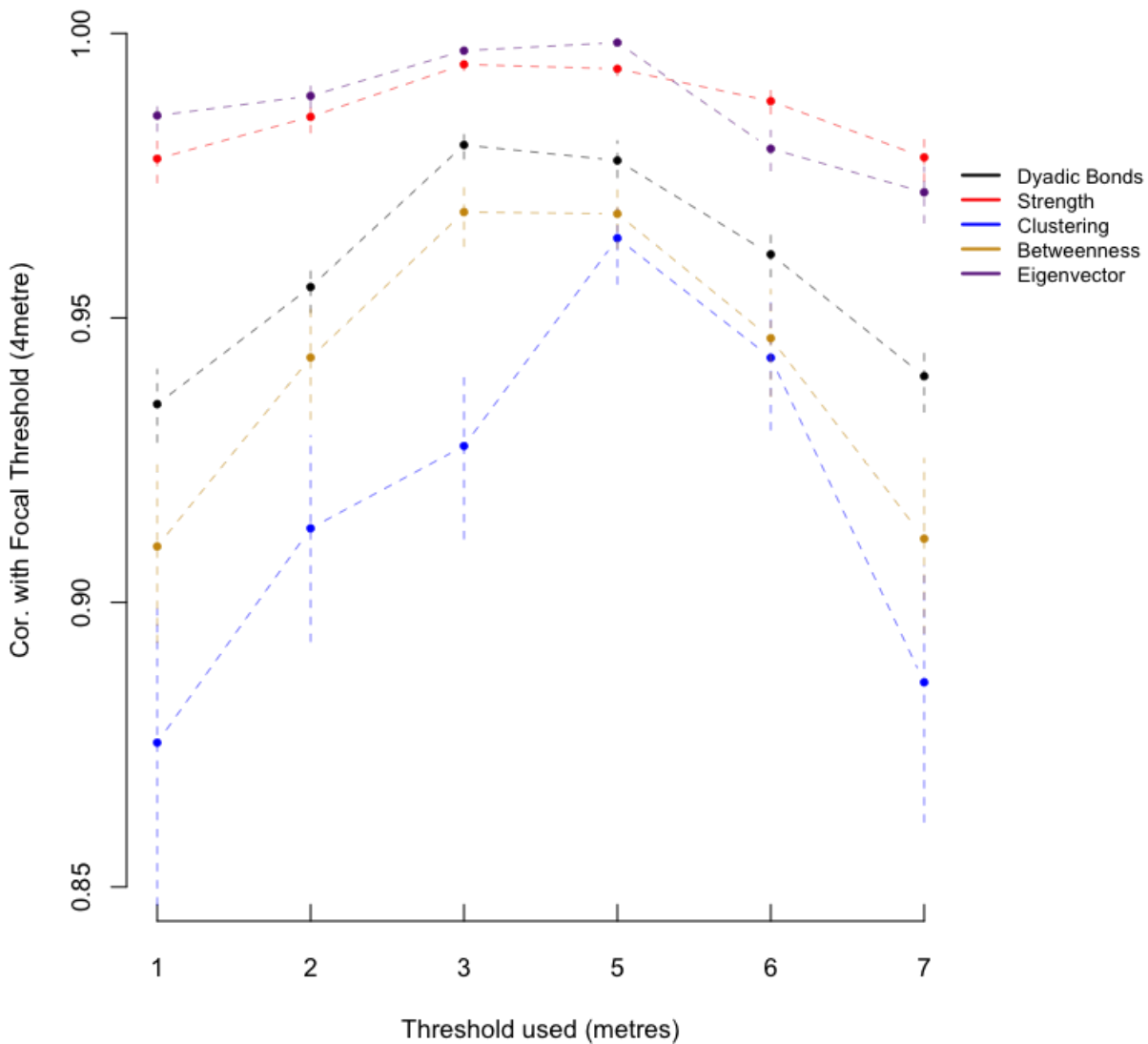


Figure S3 Similarity between the focal 4 m network (weighted by number of days seen together) with the other potential threshold distances defined using different average distances within the 5 min intervals (1-7 m thresholds). We considered the correlation in dyadic social associations scores using Mantel tests, and examined the correlation in individuals' network metrics in terms of 'weighted degree' (number of contacts with others), 'clustering coefficient' (propensity for associates to also be associated with one another), 'betweenness' (propensity to bridge the network), and 'eigenvector centrality' (the social centrality of associates). The points show the correlation and the vertical lines show the 95% confidence around this estimate.

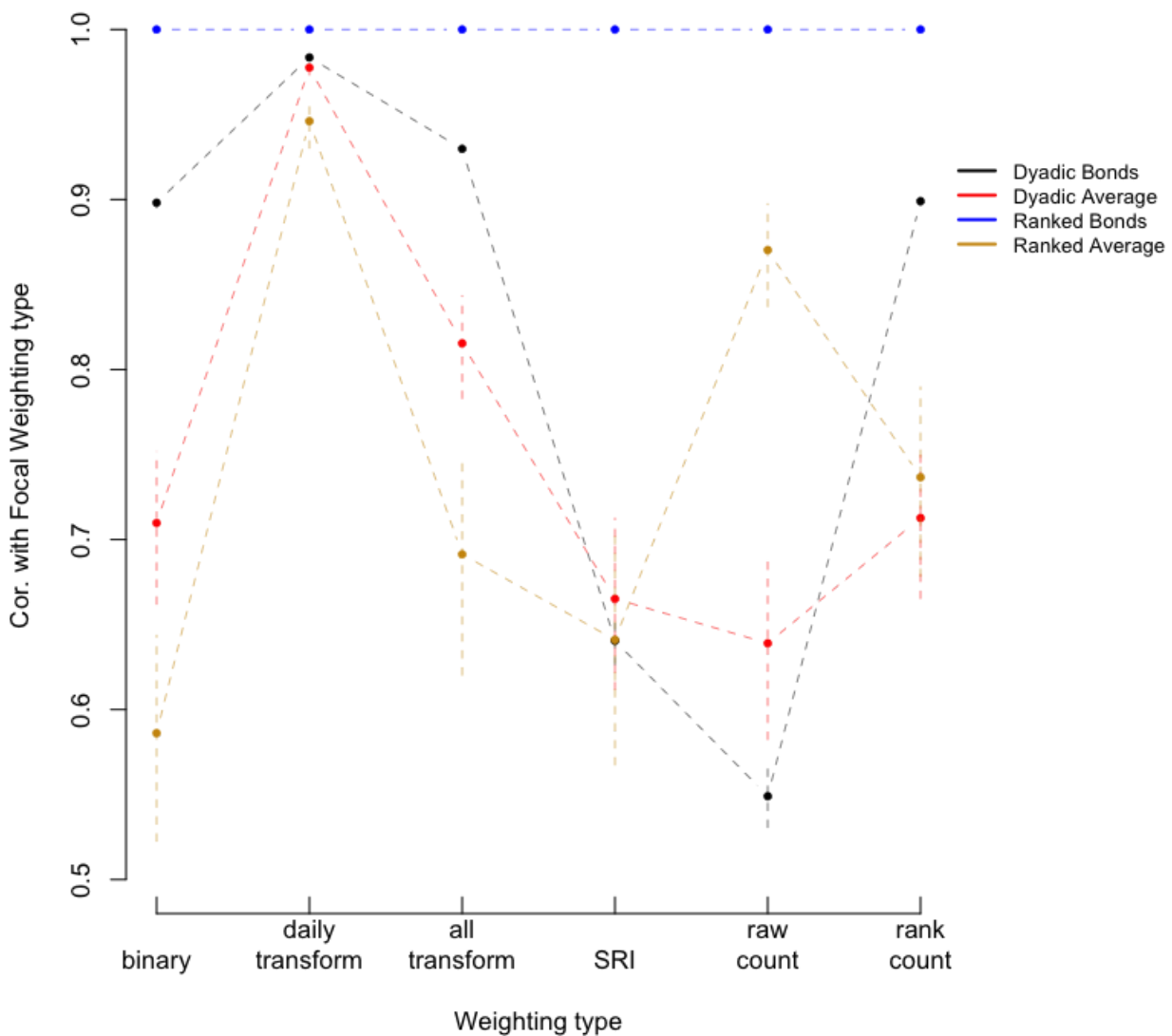


Figure S4 Similarity between the focal weighted network (weighted by number of days seen together) with the other potential weighting options specified here as ‘binary’ (whether or not individuals had social contact over the three day period), ‘daily transform’ ($1 - e^{-\text{contacts}}$ calculated for each day, where contacts = 5 min interval together each day), ‘all transform’ ($1 - e^{-\text{contacts}}$ where contacts = 5 min interval together over all of the time period), ‘SRI’ (the ‘Simple Ratio Index’ i.e. using the number of 5 min intervals each dyad was seen together but correcting for the amount of 5 min intervals both members of the dyad were seen in total), ‘raw count’ (the number of 5 min intervals each dyad was seen together), ‘rank count’ (the ranked number of 5 min intervals each dyad was seen together). We calculated the network correlations in dyadic social associations scores using Mantel tests (where ‘Dyadic bonds’ shows Pearson correlation and

'Ranked bonds' shows Spearman correlation), as well as the correlation in individuals' network metrics in terms of their average bond strength to all those they held an edge to (where 'Dyadic Average' shows Pearson correlation and 'Ranked Average' shows Spearman correlation). The points show the correlation and the vertical lines show the 95% confidence around this estimate.

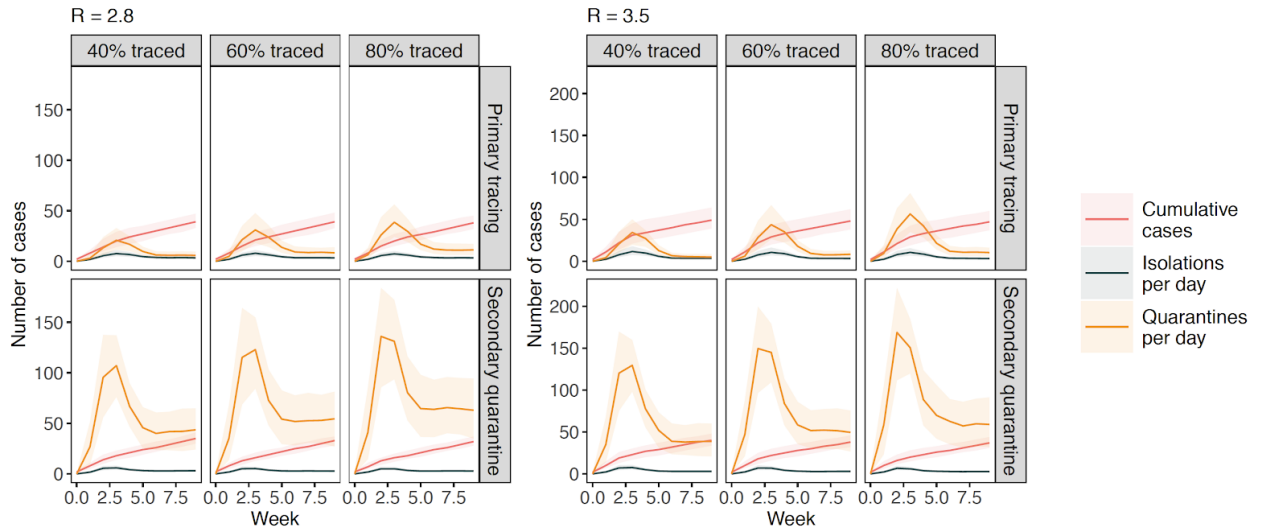


Figure S5 Epidemic model predictions of outbreak size and number of people isolated/quarantined in relation to the basic reproduction number R . Lines and shaded areas represent median and interquartile range from 1000 simulations.

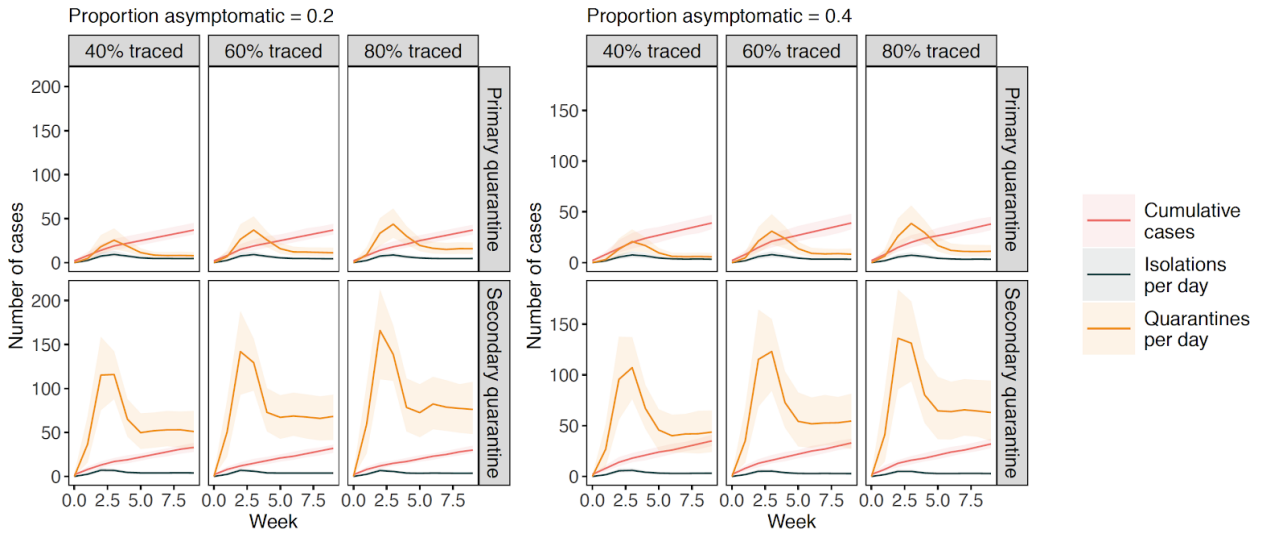


Figure S6 Epidemic model predictions of outbreak size and number of people isolated/quarantined in relation to the proportion of asymptomatic cases. Lines and shaded areas represent median and interquartile range from 1000 simulations.

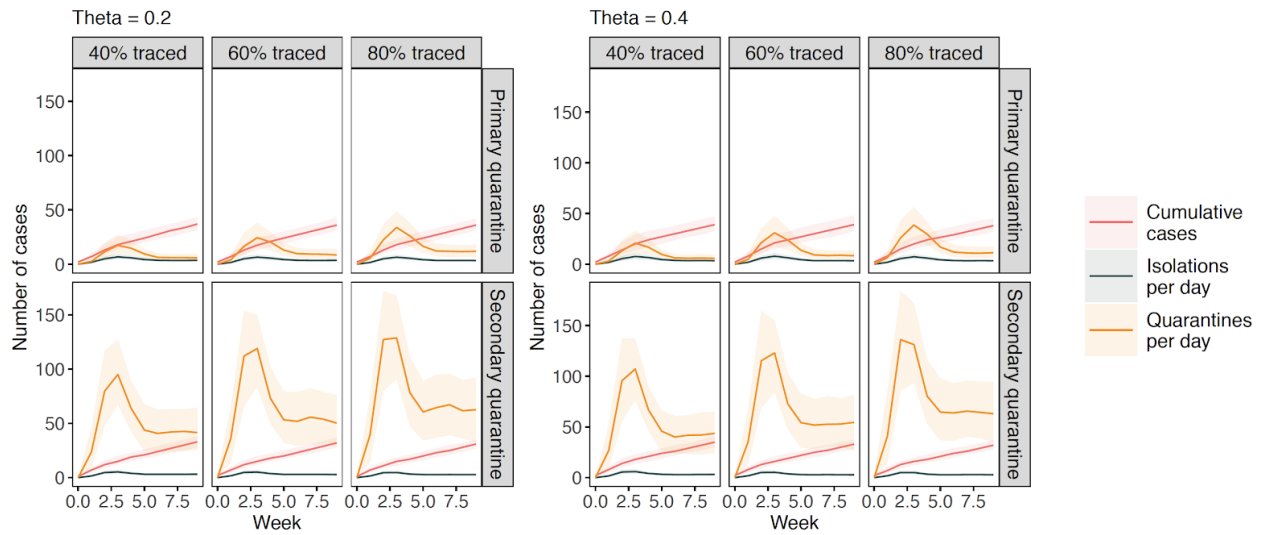


Figure S7 Epidemic model predictions of outbreak size and number of people isolated/quarantined in relation to the rate of presymptomatic transmission (theta). Lines and shaded areas represent median and interquartile range from 1000 simulations.

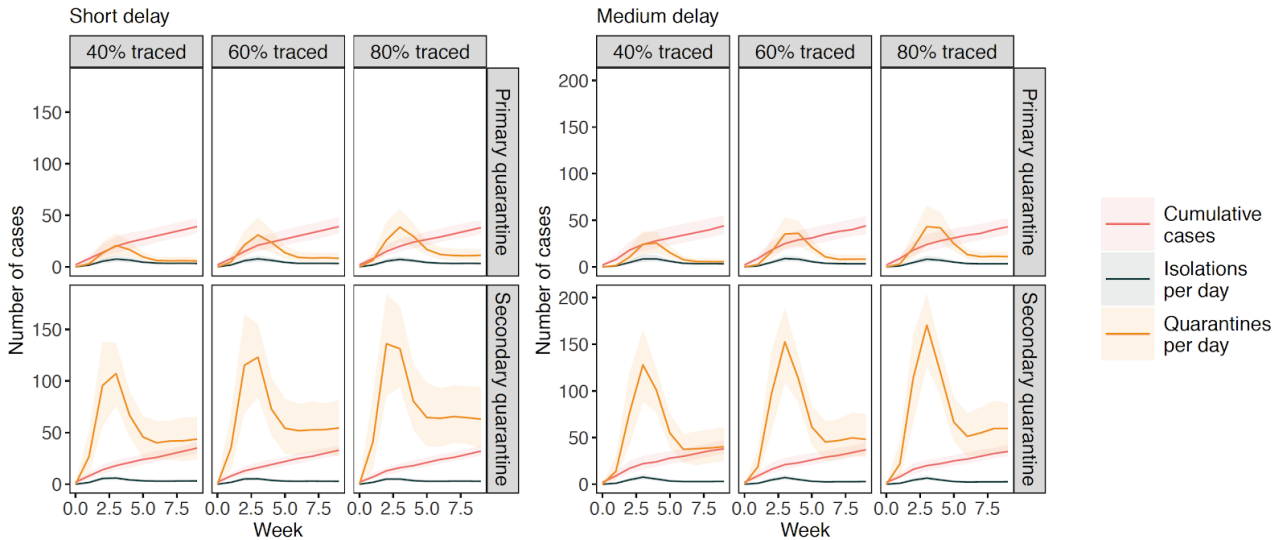


Figure S8 Epidemic model predictions of outbreak size and number of people isolated/quarantined in relation to the delay between case onset/tracing and isolation/quarantine (see methods for details). Lines and shaded areas represent median and interquartile range from 1000 simulations.

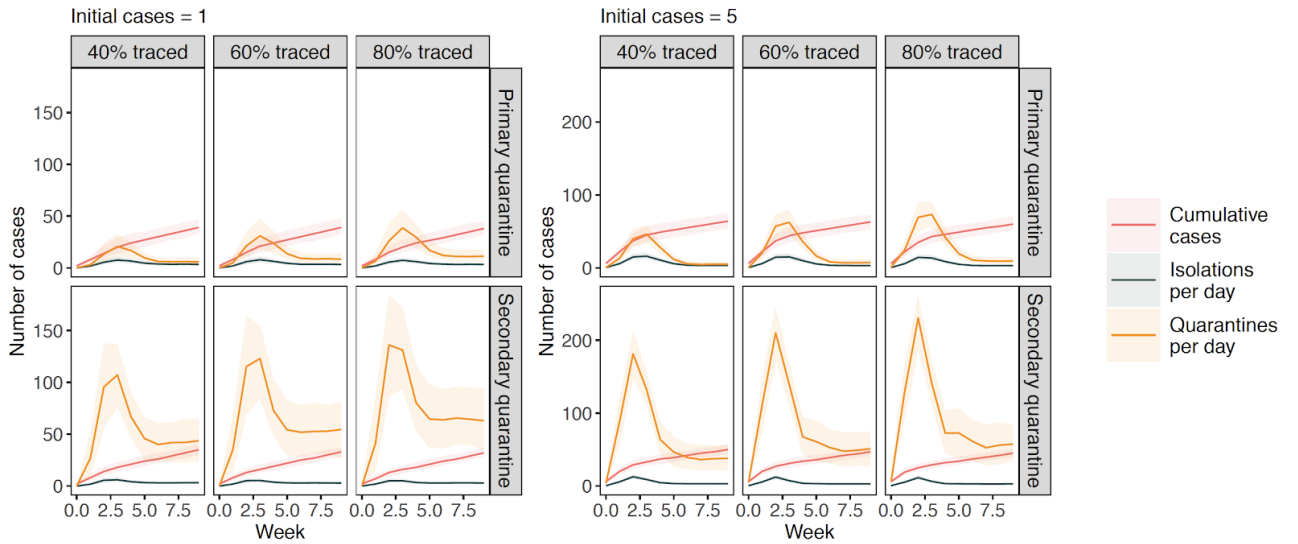


Figure S9 Epidemic model predictions of outbreak size and number of people isolated/quarantined in relation to the number of initial cases. Lines and shaded areas represent median and interquartile range from 1000 simulations.

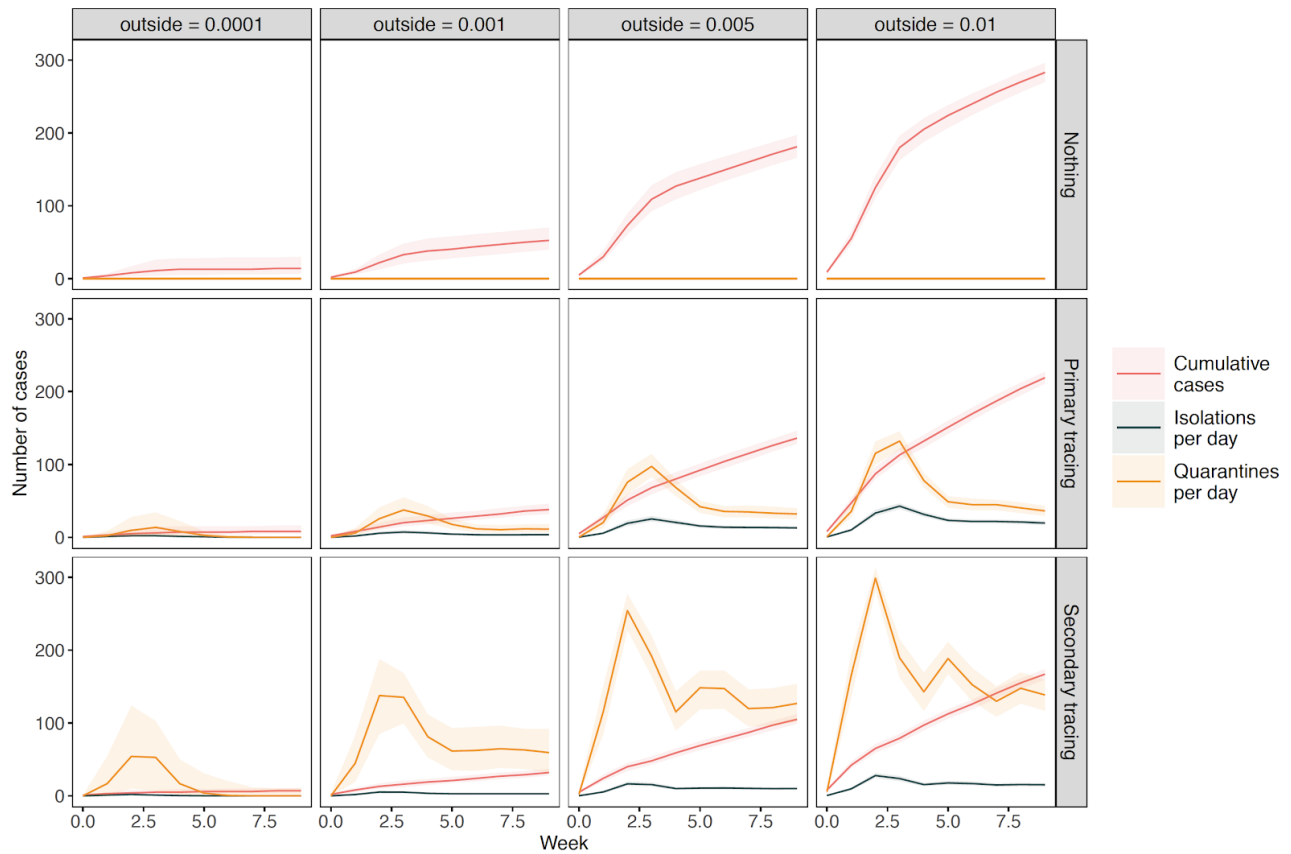


Figure S10 Epidemic model predictions of outbreak size and number of people

isolated/quarantined in relation to the outside infection rate into the Haslemere network. Outside infection rate is the probability that an individual is randomly infected on a given day (see methods for details). Lines and shaded areas represent median and interquartile range from 1000 simulations.

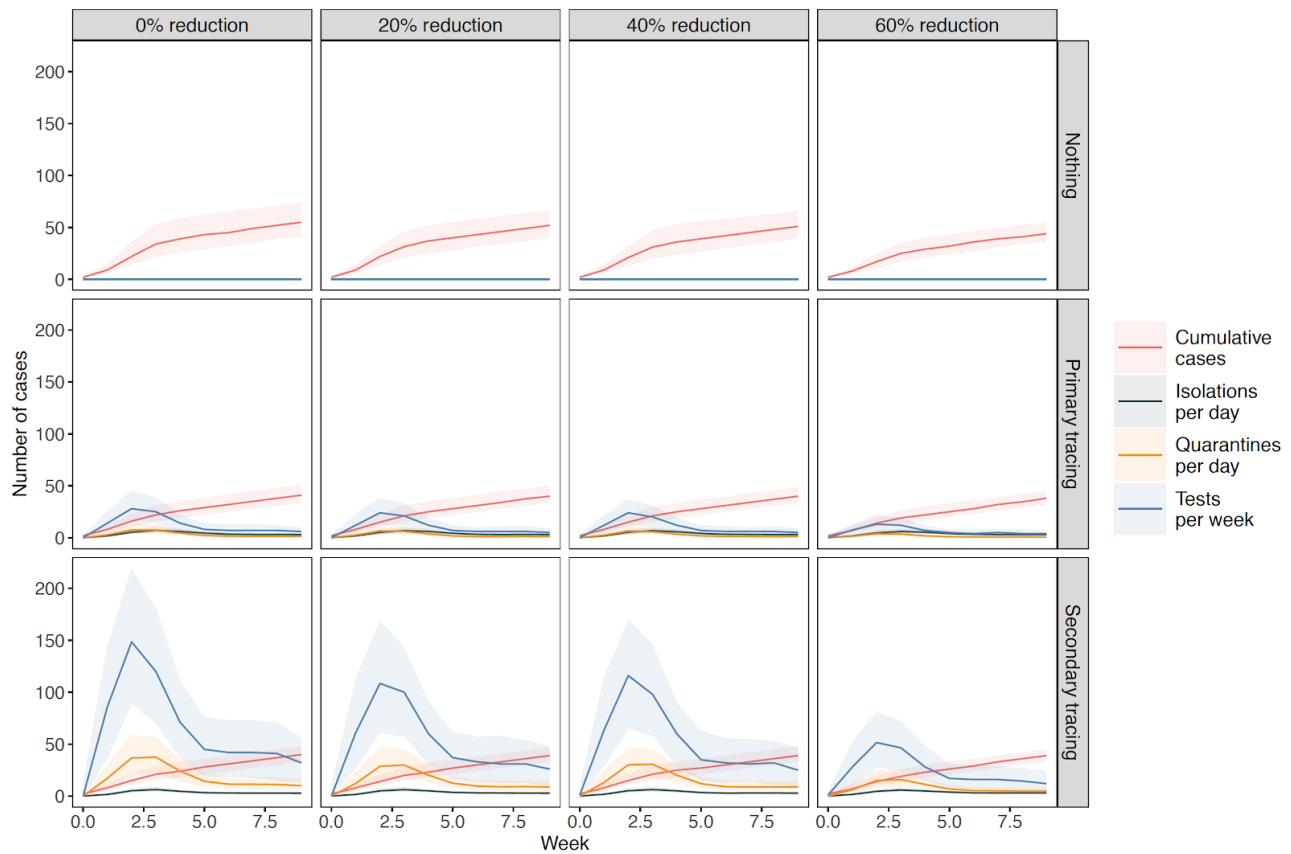


Figure S11 Epidemic model predictions of outbreak size and number of people isolated, quarantined and tested under different levels of physical distancing in the Haslemere network, with physical distancing simulated using a weighted method. The percentage reduction refers to the number of ‘weak links’ reassigned based on the amount of contact within individual days in the network, to increase clustering (see methods and Fig. S2). Tests are plotted per week rather than per day for visualisation purposes. Lines and shaded areas represent median and interquartile range from 1000 simulations.

Supplementary video 1 (separate file) Examples of case isolation, contact tracing, testing and physical distancing scenarios on COVID-19 dynamics across the Haslemere network. See Figure 1 (main text) for a full description of the network